CHAPTER SIXTEEN

Relationships Between Finite Differences and Finite Elements and Other Methods

Our explorations on the methods of finite differences and finite elements have come to an end. In Chapter 1, it was intended that the reader recognize the analogy between these two methods in one dimension. In fact, such an analogy exists for linear problems in all multidimensional geometries as long as the grid configurations are structured. In structured grids, with adjustments of the temporal parameters in generalized Galerkin methods and both temporal and convection diffusion parameters in generalized Petrov-Galerkin methods, the analogy between finite difference methods (FDM) and finite element methods (FEM) can be shown to exist also.

Traditionally, FEM equations are developed in unstructured grids as well as in structured grids. The FEM equations written in unstructured grids have global nodes irregularly connected around the entire domain, thus resulting in a large sparse matrix system, but the data management can be handled efficiently by using the element-by-element (EBS) assembly as discussed in Sections 10.3.2 and 11.5. FDM equations cannot be written in unstructured grids unless through FVM formulations. Thus, the FDM equations written only in structured grids cannot be directly compared with FEM equations written in general unstructured grids. Thus, the notion of FEM being more complicated, requiring more computer time than FDM, is an unfortunate comparison. For fair comparisons, FEM equations must be written in structured grids as in FDM.

In unstructured adaptive methods (Chapter 19), our assessments as to the merits and demerits of FDM versus FEM will be faced with a new challenge. This is because adaptive methods are instrumental in resolving many problems of numerical difficulties such as in shock waves and turbulence, making the fair comparison between FDM and FEM difficult.

Additionally, there are special numerical schemes in which both FDM and FEM are involved such as in DGM (discontinuous Galerkin methods, Section 13.5), FVM via FDM (Chapter 7), and FVM via FEM (Chapter 15). The most logical and simple comparison between FDM and FEM can be made in the flowfield-dependent variation (FDV) methods in which FDM (Section 6.5) and FEM (Section 13.6) contribute only through their unique discretization schemes, because all the physics required are already contained in the FDV equations. Indeed, it was demonstrated in Sections 6.8 and 13.7 that the choice between FDM and FEM is inconsequential if FDV equations are used.

Although the analogy between FDM and FEM is well understood, we must recognize some differences. One of the most significant differences between these two

methodologies is the variational (or weak) formulation employed in FEM, not only for the governing equations but also for all constraint conditions particularly useful for solution stability and accuracy. Any number of variational constraint conditions can be introduced and simply added to the variational forms of the governing equations. This subject was covered in Chapters 11 through 14.

Thus, in this chapter, we are first concerned with analogies between FDM and FEM, with finite element equations written only in structured grids. We begin with simple elliptic, parabolic, and hyperbolic equations, followed by non-linear, multidimensional, and unstructured grid systems.

Historically, many methods other than FDM, FEM, and FVM have been developed, which are efficient for certain types of problems in physics and engineering. They include boundary element methods (BEM), coupled Eulerian-Lagrangian (CEL) methods, particle-in-cell (PIC) methods, and Monte Carlo methods (MCM), among others. For the sake of completeness, these methods will be briefly discussed in this chapter.

16.1 SIMPLE COMPARISONS BETWEEN FDM AND FEM

(1) Elliptic Equations

Consider an elliptic equation of the form

$$\frac{\partial^2 u}{\partial x^2} + \frac{\partial^2 u}{\partial y^2} = 0 \tag{16.1.1}$$

Using the four linear triangular elements, arranged in structured grids as shown Figure 16.1.1a, the assembled 5×5 finite element equations via SGM (Section 10.1) provide the global equation at nodes corresponding to (16.1.1) as follows:

$$\frac{u_4 - 2u_5 + u_2}{\Delta x^2} + \frac{u_1 - 2u_5 + u_3}{\Delta y^2} = 0 \tag{16.1.2}$$

This is identical to the five-point FDM equation written for the case of Figure 16.1.1b.

Similarly, it can be shown that the finite element equation for either eight linear triangular elements or four linear rectangular elements written at node 5 (Figure 16.1.1c) is identical to the nine-point FDM formula (Figure 16.1.1d) as follows:

$$u_1 + u_3 + u_7 + u_9 - \frac{2(\Delta x^2 - 5\Delta y^2)}{\Delta x^2 + \Delta y^2}(u_4 + u_6) + \frac{2(5\Delta x^2 - \Delta y^2)}{\Delta x^2 + \Delta y^2}(u_2 - u_8) - 20u_5 = 0 \tag{16.1.3}$$

The solution of these equations may be carried out using the procedure of FDM such as Jacobi iteration method, point Gauss-Seidel iteration, line Gauss-Seidel iteration, point successive over-relaxation, line successive relaxation, or alternating direction implicit (ADI) method, as discussed in Chapter 4.

(2) Parabolic Equations

A typical parabolic equation is given by

$$\frac{\partial u}{\partial t} - \alpha \frac{\partial^2 u}{\partial x^2} = 0 \tag{16.1.4}$$

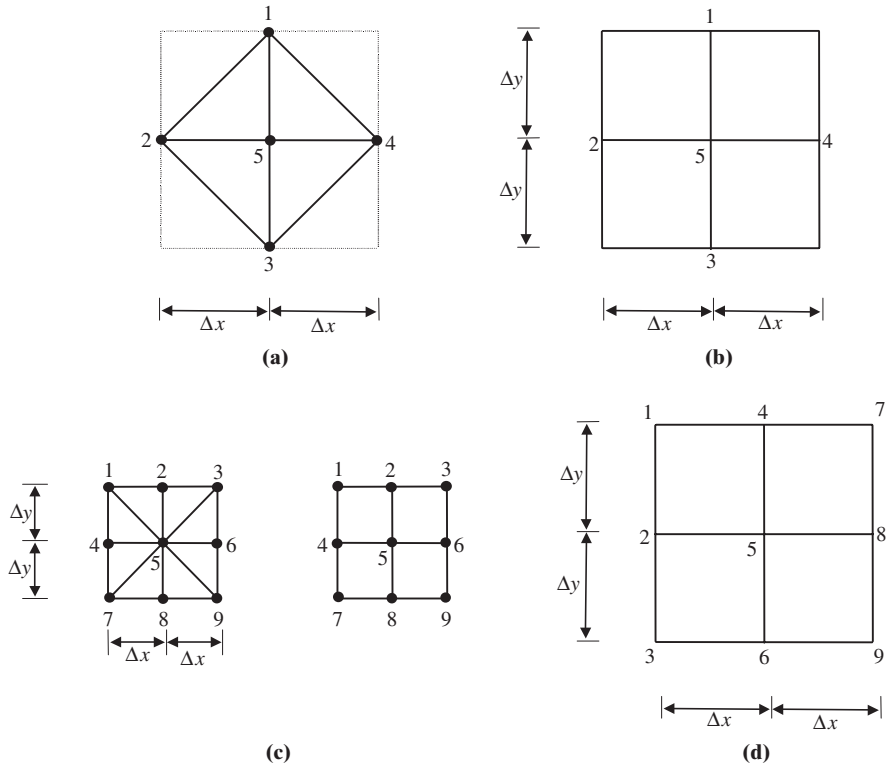

Figure 16.1.1 Analogy between FEM and FDM. **(a)** 4×4 finite element equations. **(b)** 5-point finite difference equations. **(c)** 9×9 finite element equations. **(d)** 9-point finite difference equations.

The finite element equations using GGM (Section 10.2) with linear approximations are of the form

$$(A_{\alpha\beta} + \eta \Delta t K_{\alpha\beta}) u_\beta^{n+1} = [A_{\alpha\beta} + (1-\eta)\Delta t K_{\alpha\beta}] u_\beta^n$$

where the Neumann boundary conditions are assumed to vanish. The local element stiffness matrix and lumped mass matrix are, respectively,

$$K_{NM}^{(e)} = \frac{1}{\Delta x} \begin{bmatrix} 1 & -1 \\ -1 & 1 \end{bmatrix}$$

$$A_{NM}^{(e)} = \frac{\Delta x}{2} \begin{bmatrix} 1 & 0 \\ 0 & 1 \end{bmatrix}$$

Here, the lumped mass matrix is used instead of the consistent mass matrix in order to arrive at the results identical to the finite difference equations.

Assembly of two equal elements with three nodes leads to the global finite element equation for the center node i in terms of the end nodes $i-1$ and $i+1$, with $\eta = 0$:

$$u_i^{n+1} = u_i^n + d\left(u_{i+1}^n - 2u_i^n + u_{i-1}^n\right) \tag{16.1.5}$$

This is an explicit scheme known as FTCS finite difference formula.

The Crank-Nicolson scheme, a well-known implicit scheme is obtained with $\eta = 1/2$,

$$u_i^{n+1} = u_i^n + \frac{\alpha \Delta t}{2\Delta x^2}\left[\left(u_{i+1}^{n+\frac{1}{2}} - 2u_i^{n+\frac{1}{2}} + u_{i-1}^{n+\frac{1}{2}}\right) + \left(u_{i+1}^n - 2u_i^n + u_{i-1}^n\right)\right] \tag{16.1.6}$$

It is now obvious that with appropriate choices of $\eta(0 \le \eta \le 1)$ many other FDM formulas can be derived. Therefore, the solution procedures as used in FDM such as DuFort-Frankel, Laasonen, β-method, fractional step methods, or ADI methods arise, which were discussed in Section 4.2.

(3) Hyperbolic Equations

For illustration, let us examine the first order hyperbolic equation of the form

$$\frac{\partial u}{\partial t} + a\frac{\partial u}{\partial x} = 0 \tag{16.1.7}$$

Recall that SGM and GGM were used to deal with elliptic equations and parabolic equations, respectively. For hyperbolic equations, however, we must invoke a convection test function in addition to the standard test function to cope with possible physical discontinuities. In this case, we resort to GPG (Section 11.3) and write

$$\int_0^1 W(\xi)\left[\int \Phi_\alpha\left(\frac{\partial u}{\partial t} + a\frac{\partial u}{\partial x}\right)dx + \int \Psi_\alpha\left(a\frac{\partial u}{\partial x}\right)dx\right]d\xi = 0 \tag{16.1.8}$$

or

$$[A_{\alpha\beta} + \eta\Delta t(B_{\alpha\beta} + C_{\alpha\beta})]u_\beta^{n+1} = [A_{\alpha\beta} - (1-\eta)\Delta t(B_{\alpha\beta} + C_{\alpha\beta})]u_\beta^n \tag{16.1.9}$$

For two elements with three nodes with lumped mass, we obtain

$$\begin{aligned}
&\left\{\frac{\Delta x}{2}\begin{bmatrix}1&0&0\\0&2&0\\0&0&1\end{bmatrix} + \frac{\eta\Delta ta}{2}\begin{bmatrix}-1&1&0\\-1&0&1\\0&-1&1\end{bmatrix} + \eta\Delta ta\alpha\begin{bmatrix}1&-1&0\\-1&2&-1\\0&-1&1\end{bmatrix}\right\}\begin{bmatrix}u_1\\u_2\\u_3\end{bmatrix}^{n+1} \\
&\quad = \left\{\frac{\Delta x}{2}\begin{bmatrix}1&0&0\\0&2&0\\0&0&1\end{bmatrix} - (1-\eta)\frac{\Delta ta}{2}\begin{bmatrix}-1&1&0\\-1&0&1\\0&-1&1\end{bmatrix}\right. \\
&\qquad \left. + (1-\eta)\Delta ta\alpha\begin{bmatrix}1&-1&0\\-1&2&-1\\0&-1&1\end{bmatrix}\right\}\begin{bmatrix}u_1\\u_2\\u_3\end{bmatrix}^n
\end{aligned}$$

Expanding at node 2 or i in terms of $i-1$ and $i+1$ nodes, we have

$$\begin{aligned}
&u_i^{n+1} + \eta\frac{\Delta ta}{\Delta x}\left[\left(\frac{1}{2} - \alpha\right)u_{i+1} + 2\alpha u_i - \left(\frac{1}{2} + \alpha\right)u_{i-1}\right]^{n+1} \\
&\quad = u_i^n - (1-\eta)\frac{\Delta ta}{\Delta x}\left[\left(\frac{1}{2} - \alpha\right)u_{i+1} + 2\alpha u_i - \left(\frac{1}{2} + \alpha\right)u_{i-1}\right]^n
\end{aligned} \tag{16.1.10}$$

With appropriate choices of the temporal parameter $\eta(0 \le \eta \le 1)$ and the convection parameter $\alpha(a \le \alpha \le b)$ with a and b satisfying both the stability and accuracy criteria (11.3.20, 11.3.22), we arrive at various finite difference schemes.

With $\eta = 0$ and $\alpha = 1/2$ we obtain the FTBS scheme,

$$\frac{u_i^{n+1} - u_i^n}{\Delta t} = -a\frac{\left(u_i^n - u_{i-1}^n\right)}{\Delta x} \tag{16.1.11}$$

To demonstrate that the Lax-Wendroff scheme can be derived, we begin with the Taylor Series expansion of (16.1.7) in the form

$$u_i^{n+1} = u_i^n - a\Delta t\frac{\partial u}{\partial x} + \frac{(a\Delta t)^2}{2}\frac{\partial^2 u}{\partial x^2} \tag{16.1.12}$$

or the equivalent partial differential equation,

$$\frac{\partial u}{\partial t} = -a\frac{\partial u}{\partial x} + \frac{a^2\Delta t}{2}\frac{\partial^2 u}{\partial x^2} \tag{16.1.13}$$

The GPG formulation of (16.1.13) leads to

$$\int \Phi_\alpha\left(\frac{\partial u}{\partial t} + a\frac{\partial u}{\partial x} - \frac{a^2\Delta t}{2}\frac{\partial^2 u}{\partial x^2}\right)dx + \int \Psi_\alpha\left(a\frac{\partial u}{\partial x}\right)dx = 0 \tag{16.1.14}$$

Integrating by parts and rearranging, we obtain

$$\begin{aligned} &u_i^{n+1} + \eta\frac{\Delta t a}{\Delta x}\left[\left(\frac{1}{2} - \alpha\right)u_{i+1} + 2\alpha u_i - \left(\frac{1}{2} + \alpha\right)u_{i-1}\right]^{n+1} \\ &\quad - \eta a^2\frac{\Delta t}{2\Delta x^2}(u_{i+1} - 2\alpha u_i + u_{i-1})^{n+1} = u_i^n - (1-\eta)\frac{\Delta t a}{\Delta x}\left[\left(\frac{1}{2} - \alpha\right)u_{i+1}\right. \\ &\quad \left. + 2\alpha u_i - \left(\frac{1}{2} + \alpha\right)u_{i-1}\right]^n + a^2\frac{\Delta t}{2\Delta x^2}(u_{i+1} - 2\alpha u_i + u_{i-1})^n \end{aligned} \tag{16.1.15}$$

For $\eta = 0$ and $\alpha = 0$, (16.1.15) becomes

$$u_i^{n+1} = u_i^n - \frac{a\Delta t}{2\Delta x}\left(u_{i+1}^n - u_{i-1}^n\right) + \frac{(a\Delta t)^2}{2\Delta x^2}\left(u_{i+1}^n - 2u_i^n - u_{i-1}^n\right) \tag{16.1.16}$$

This is identical to the explicit Lax-Wendroff scheme presented in (4.3.15).

Implicit schemes such as Euler FTCS and Crank-Nicolson are generated as follows:

Euler FTCS ($\eta = 1$ *and* $\alpha = 0$)

$$\frac{u_i^{n+1} - u_i^n}{\Delta t} = -\frac{a\left(u_{i+1}^{n+1} - u_{i-1}^{n+1}\right)}{2\Delta x} \tag{16.1.17}$$

Crank-Nicolson ($\eta = 1/2$ *and* $\alpha = 0$)

$$\frac{u_i^{n+1} - u_i^n}{\Delta t} = -\frac{a}{2}\left[\frac{\left(u_{i+1}^{n+1} - u_{i-1}^{n+1}\right)}{2\Delta x} + \frac{\left(u_{i+1}^n - u_{i-1}^n\right)}{2\Delta x}\right] \tag{16.1.18}$$

Obviously, many other difference schemes can be derived using the unlimited rages of η and α through the GPG formulations. Once the finite element equations are obtained in the form analogous to finite difference equations, then the FDM solution procedure can be followed as long as structured grid configurations are used.

16.2 RELATIONSHIPS BETWEEN FDM AND FDV

It was suggested in Section 6.5 that almost all existing FDM schemes can arise from the FDV scheme. We examine the analogies of FDV to some of the FDM schemes in this section.

Referring to (6.5.13 or 13.6.2) with the source terms neglected, we write

$$\left\{\mathbf{I}+\Delta t\,(s_1\mathbf{a}_i+s_3\mathbf{b}_i)\frac{\partial}{\partial x_i}+\left[\Delta t s_3\mathbf{c}_{ij}-\frac{\Delta t^2}{2}s_2(\mathbf{a}_i\mathbf{a}_j+\mathbf{b}_i\mathbf{a}_j)\right.\right.$$
$$\left.\left.-\frac{\Delta t^2}{2}s_4(\mathbf{a}_i\mathbf{b}_j+\mathbf{b}_i\mathbf{b}_j)\right]\frac{\partial^2}{\partial x_i\partial x_j}\right\}\Delta\mathbf{U}^{n+1}=-\frac{\Delta t}{2}\left(\frac{\partial\mathbf{F}_i^n}{\partial x_i}+\frac{\partial\mathbf{G}_i^n}{\partial x_i}\right)$$
$$+\frac{\Delta t^2}{2}(\mathbf{a}_i+\mathbf{b}_i)\frac{\partial}{\partial x_i}\left(\frac{\partial\mathbf{F}_j^n}{\partial x_j}+\frac{\partial\mathbf{G}_j^n}{\partial x_j}\right) \tag{16.2.1}$$

where the Jacobians $\mathbf{a}_i$, $\mathbf{b}_i$, $\mathbf{c}_{ij}$, are flowfield dependent, but held constant within a discrete numerical integration time and updated for each successive time step. Here, (16.2.1) is regarded as the most general form which may be reduced to other CFD schemes in FDM and FEM.

(1) Beam-Warming Scheme

To show that a simplified special case of (16.2.1) resembles one of the most popular FDM schemes, let us express the Beam-Warming [1978] method using the notation of FDV,

$$\left\{\mathbf{I}+\frac{\theta\Delta t}{1+\xi}\left[\frac{\partial}{\partial x_i}(\mathbf{a}_i+\mathbf{b}_i)+\frac{\partial^2\mathbf{c}_{ij}}{\partial x_i\partial x_j}\right]\right\}\Delta\mathbf{U}^{n+1}$$
$$=\frac{\Delta t}{1+\xi}\left(\frac{\partial\mathbf{F}_i^n}{\partial x_i}+\frac{\partial\mathbf{G}_i^n}{\partial x_i}\right)+\frac{\theta\Delta t}{1+\xi}\frac{\partial\mathbf{G}_i^n}{\partial x_i}+\frac{\xi}{1+\xi}\Delta\mathbf{U}^n \tag{16.2.2}$$

with $0\le(\theta,\xi)\le 1$. It is seen that the analogy of FDV to the Beam-Warming scheme is readily evident, although the main difference is that the parameters θ and ξ are chosen arbitrarily instead of being flowfield-dependent.

In general, the FDV scheme can be written in the form (6.5.14 or 13.6.9),

$$\left(\mathbf{I}+\mathbf{E}_i^n\frac{\partial}{\partial x_i}+\mathbf{E}_{ij}^n\frac{\partial^2}{\partial x_i\partial x_j}\right)\Delta\mathbf{U}^{n+1}=-\mathbf{Q}^n \tag{16.2.3}$$

The Beam-Warming scheme and other related schemes such as Euler explicit, Euler implicit, three-point implicit, trapezoidal implicit, and leapfrog explicit schemes are summarized in Table 16.2.1.

Other schemes of FDM are compared with FDV as follows:

(2) Lax-Wendroff Scheme

The Lax-Wendroff scheme without artificial viscosity takes the form

$$\Delta\mathbf{U}_i^{n+1}=-\frac{\Delta t}{\Delta x}\left(\mathbf{F}_{i+\frac{1}{2}}-\mathbf{F}_{i-\frac{1}{2}}\right)-\frac{\Delta t^2}{2\Delta x^2}\left[\mathbf{a}_{i+\frac{1}{2}}\mathbf{F}_{i+1}-\left(\mathbf{a}_{i+\frac{1}{2}}-\mathbf{a}_{i-\frac{1}{2}}\right)\mathbf{F}_i+\mathbf{a}_{i-\frac{1}{2}}\mathbf{F}_{i-1}\right] \tag{16.2.4}$$

Table 16.2.1 Comparison of FDV with Beam-Warming and Related Schemes

	s_1	s_3	E_I	E_{ij}	Q^n	Truncation Error
Beam-Warming [1]	$\frac{\theta}{1+\xi}$	$\frac{\theta}{1+\xi}$	$\frac{\theta\Delta t}{1+\xi}(\mathbf{a}_i+\mathbf{b}_i)$	$\frac{\theta\Delta t}{1+\xi}\mathbf{c}_{ij}$	$\frac{\Delta t}{1+\xi}\mathbf{W}^n+\frac{\xi}{1+\xi}\Delta\mathbf{U}^n$	$O\left[(\theta-\frac{1}{2}-\xi)\,\Delta t^2, \Delta t^3\right]$
Euler explicit	0	0	*	*	*	$O(\Delta t^2)$
Euler implicit	1	1	*	*	*	$O(\Delta t^2)$
Three-point implicit	2/3	2/3	*	*	*	$O(\Delta t^3)$
Trapezoidal implicit	1/2	1/2	*	*	*	$O(\Delta t^3)$
Leap frog explicit	0	0	*	*	*	$O(\Delta t^3)$

* Not applicable

This scheme arises if we set in FDV,

$$\mathbf{a}_{i+\frac{1}{2}}=\mathbf{a}_{i-\frac{1}{2}}=\mathbf{a}, \qquad s_1=0, \qquad s_2=0, \qquad s_3=0, \qquad s_4=0$$

(3) Lax-Wendroff Scheme with Viscosity

The Lax-Wendroff scheme with artificial viscosity is given by

$$\Delta\mathbf{U}_i^{n+1}=-\frac{\Delta t}{\Delta x}\left(\mathbf{F}_{i+\frac{1}{2}}-\mathbf{F}_{i-\frac{1}{2}}\right) \tag{16.2.5}$$

with

$$\mathbf{F}_{i+\frac{1}{2}}=\frac{\mathbf{F}_{i+1}+\mathbf{F}_i}{2}-\frac{\Delta t}{2\Delta x}\mathbf{a}_{i+\frac{1}{2}}(\mathbf{F}_{i+1}-\mathbf{F}_i)+D_{i+\frac{1}{2}}(\mathbf{U}_{i+1}-\mathbf{U}_i)$$

$$\mathbf{F}_{i-\frac{1}{2}}=\frac{\mathbf{F}_i+\mathbf{F}_{i-1}}{2}-\frac{\Delta t}{2\Delta x}\mathbf{a}_{i-\frac{1}{2}}(\mathbf{F}_i-\mathbf{F}_{i-1})+D_{i-\frac{1}{2}}(\mathbf{U}_i-\mathbf{U}_{i-1})$$

This scheme arises if we set

$$D_{i+\frac{1}{2}}=D_{i-\frac{1}{2}}=\mathbf{a}s_1, \qquad s_2=0, \qquad s_3=0, \qquad s_4=0$$

This implies that the artificial viscosity is proportional to the FDV parameter s_1, but here it is manually implemented in the Lax-Wendroff scheme.

(4) Explicit MacCormack Scheme

Combining the predictor corrector steps of the MacCormack scheme, we write

$$\begin{aligned}\Delta\mathbf{U}_i^{n+1}&=-\frac{\Delta t}{\Delta x}\left(\mathbf{F}_{i+1}^n-\mathbf{F}_i^n\right)-\frac{\Delta t}{\Delta x}(\mathbf{F}_i^*-\mathbf{F}_{i-1}^*)+D_i\\&=-\frac{\Delta t}{\Delta x}\left(\mathbf{F}_{i+1}^n-\mathbf{F}_i^n\right)-\frac{\Delta t}{\Delta x}\left(\mathbf{F}_{i+\frac{1}{2}}-\mathbf{F}_{i-\frac{1}{2}}\right)\\&\quad-\frac{\Delta t^2}{\Delta x^2}\left[\mathbf{a}_{i+\frac{1}{2}}\mathbf{F}_{i+1}-\left(\mathbf{a}_{i+\frac{1}{2}}+\mathbf{a}_{i-\frac{1}{2}}\right)\mathbf{F}_i+\mathbf{a}_{i-\frac{1}{2}}\mathbf{F}_{i-1}\right]+D_i\end{aligned} \tag{16.2.6}$$

The FDV becomes identical to this scheme with the following adjustments:

$$\mathbf{a}_{i+\frac{1}{2}} = \mathbf{a}_{i-\frac{1}{2}} = \mathbf{a}$$
$$\mathbf{F}_i^n - \mathbf{F}_{i-1}^n = \mathbf{F}_{i+1}^n - \mathbf{F}_i^n + \mathbf{F}_{i+\frac{1}{2}} - \mathbf{F}_{i-\frac{1}{2}}$$
$$s_1 = 0, \qquad s_2 = 0, \qquad s_3 = 0, \qquad s_4 = 0$$

and the s_2 term in the FDV method is equivalent to

$$D_i = \frac{\omega}{8}\left(\mathbf{U}_{i+\frac{1}{2}}^n - 4\mathbf{U}_{i+1}^n + 6\mathbf{U}_i^n - 4\mathbf{U}_{i-1}^n + \mathbf{U}_{i-2}^n\right)$$

This again is a manifestation that shows the equivalent of the s_2 terms is manually supplied in the MacCormack method.

(5) First Order Upwind Scheme

This scheme is written as

$$\begin{aligned}\Delta\mathbf{U}_i^{n+1} &= -\frac{\Delta t}{\Delta x}\left(\mathbf{F}_{i+\frac{1}{2}}^* - \mathbf{F}_{i-\frac{1}{2}}^*\right)\\ &= -\frac{\Delta t}{\Delta x}\left\{\left[\frac{1}{2}\left(\mathbf{F}_i^n + \mathbf{F}_{i+1}^n\right) - \frac{1}{2}|\mathbf{a}|\left(\mathbf{U}_{i+1}^n - \mathbf{U}_i^n\right)\right]\right.\\ &\quad \left. - \left[\frac{1}{2}\left(\mathbf{F}_i^n + \mathbf{F}_{i-1}^n\right) - \frac{1}{2}|\mathbf{a}|\left(\mathbf{U}_i^n - \mathbf{U}_{i-1}^n\right)\right]\right\} \qquad (16.2.7)\end{aligned}$$

The FDM analogy is obtained by setting

$$\mathbf{F}_i^n = \frac{1}{2}\mathbf{F}_{i+1}^n, \qquad \mathbf{F}_{i-1}^n = \frac{1}{2}\mathbf{F}_{i-1}^n$$
$$s_2\mathbf{a}C\left(\Delta\mathbf{U}_i^{n+1} - 2\Delta\mathbf{U}_{i-1}^{n+1} + \Delta\mathbf{U}_{i-2}^{n+1}\right) = |\mathbf{a}|\left(\mathbf{U}_{i+1}^n - \mathbf{U}_{i-1}^n\right)$$

where C is the Courant number.

(6) Implicit MacCormack Scheme

With all second order derivatives removed from (16.2.1), we obtain the implicit MacCormack scheme by setting $s_1 = 1, s_2 = 0, s_3 = 0, s_4 = 0$. However, it is necessary to divide the process into the predictor and corrector steps. Once again the flowfield-dependent variation parameters for FDV will allow the computation to be performed in a single step.

(7) TVD Scheme

Another example is the analogy of FDV-FDM to the FDM-TVD scheme. To see this, we write (6.5.13) in one dimension using linear trial and test functions with all Neumann boundary conditions neglected.

$$\begin{aligned}&\frac{1}{6\Delta t}\left(\Delta\mathbf{U}_{i+1}^{n+1} + 4\Delta\mathbf{U}_i^{n+1} + \Delta\mathbf{U}_{i-1}^{n+1}\right) = \frac{1}{2\Delta x}(s_1\mathbf{a} + s_3\mathbf{b})\left(\Delta\mathbf{U}_{i+1}^{n+1} - \Delta\mathbf{U}_{i-1}^{n+1}\right)\\ &\quad + \frac{1}{2\Delta x^2}\{2s_3\mathbf{c} - \Delta t[s_2(\mathbf{a}^2 + \mathbf{ab}) + s_4(\mathbf{ba} + \mathbf{b}^2)]\}\left(\Delta\mathbf{U}_{i+1}^{n+1} - 2\Delta\mathbf{U}_i^{n+1} + \Delta\mathbf{U}_{i-1}^{n+1}\right)\\ &\quad + \frac{1}{2\Delta x}\left(\mathbf{F}_{i+1}^n - \mathbf{F}_{i-1}^n + \mathbf{G}_{i+1}^n - \mathbf{G}_{i-1}^n\right) - \frac{\Delta t}{2\Delta x^2}(\mathbf{a} + \mathbf{b})\\ &\quad \times\left(\mathbf{F}_{i+1}^n - 2\mathbf{F}_i^n + \mathbf{F}_{i-1}^n + \mathbf{G}_{i+1}^n - 2\mathbf{G}_i^n + \mathbf{G}_{i-1}^n\right) \qquad (16.2.8)\end{aligned}$$

Neglecting all diffusion terms, adopting a lumped mass system, and moving one nodal point upstream, we have

$$\frac{\Delta \mathbf{U}_i^{n+1}}{\Delta t} = \frac{s_1 \mathbf{a}}{\Delta x}\left(\Delta \mathbf{U}_i^{n+1} - \Delta \mathbf{U}_{i-1}^{n+1}\right) - \frac{s_2 \mathbf{a}^2 \Delta t}{2\Delta x^2}\left(\Delta \mathbf{U}_i^{n+1} - 2\Delta \mathbf{U}_{i-1}^{n+1} + \Delta \mathbf{U}_{i-2}^{n+1}\right) + \frac{1}{\Delta x}\left(\mathbf{F}_i^n - \mathbf{F}_{i-1}^n\right) - \frac{\mathbf{a}\Delta t}{2\Delta x^2}\left(\mathbf{F}_i^n - 2\mathbf{F}_{i-1}^n + \mathbf{F}_{i-2}^n\right) \tag{16.2.9}$$

The FDM-TVD for the 1-D Euler equation is written as

$$\frac{d\,\mathbf{U}_i}{dt} = -\frac{\mathbf{a}^+}{\Delta x}\left[(\mathbf{U}_i - \mathbf{U}_{i-1}) + \frac{1}{2}\Psi^+_{i-\frac{1}{2}}(\mathbf{U}_i - \mathbf{U}_{i-1}) - \frac{1}{2}\Psi^+_{i-\frac{3}{2}}(\mathbf{U}_{i-1} - \mathbf{U}_{i-2})\right] - \frac{\mathbf{a}^-}{\Delta x}\left[(\mathbf{U}_{i+1} - \mathbf{U}_i) + \frac{1}{2}\Psi^-_{i+\frac{1}{2}}(\mathbf{U}_{i+1} - \mathbf{U}_i) - \frac{1}{2}\Psi^-_{i+\frac{3}{2}}(\mathbf{U}_{i+2} - \mathbf{U}_{i+1})\right] \tag{16.2.10}$$

with

$$\mathbf{a}^+ = \max(0,\mathbf{a}) = \frac{1}{2}(\mathbf{a} + |\mathbf{a}|)$$

$$\mathbf{a}^- = \min(0,\mathbf{a}) = \frac{1}{2}(\mathbf{a} - |\mathbf{a}|)$$

Introducing variation parameter s for the time derivative on the right-hand side of (16.2.10) the form

$$\mathbf{U}_i = \mathbf{U}_i^n + s\,\Delta \mathbf{U}_i^{n+1} \tag{16.2.11}$$

Substituting (16.2.11) into (16.2.10) and assuming that

$$\mathbf{a}^- = 0, \qquad \mathbf{a}^+ = \mathbf{a}, \qquad \Psi^+_{i-\frac{1}{2}} = \Psi^+_{i-\frac{3}{2}} = \Psi$$

we obtain

$$\frac{\Delta \mathbf{U}_i^{n+1}}{\Delta t} = \frac{s\mathbf{a}}{2\Delta x}\left(\Delta \mathbf{U}_i^{n+1} - \Delta \mathbf{U}_{i-1}^{n+1}\right) - \frac{s\Psi \mathbf{a}\Delta x}{2\Delta x^2}\left(\Delta \mathbf{U}_i^{n+1} - 2\Delta \mathbf{U}_{i-1}^{n+1} + \Delta \mathbf{U}_{i-2}^{n+1}\right) - \frac{1}{\Delta x}\left(\mathbf{F}_i^n - \mathbf{F}_{i-1}^n\right) - \frac{\Psi \Delta x}{2\Delta x^2}\left(\mathbf{F}_i^n - 2\mathbf{F}_{i-1}^n + \mathbf{F}_{i-2}^n\right) \tag{16.2.12}$$

Comparing (16.2.9) and (16.2.12) reveals that, with

$$s_1 = -\frac{s}{2}, \qquad s_2 = \frac{s\Delta x \Psi}{\mathbf{a}\Delta t}$$

and -1 for the coefficient of $(\mathbf{F}_i^n - \mathbf{F}_{i-1}^n)$ term, we note that the FDV-FDM formulation and FDM-TVD scheme are analogous; in fact, they are identical under the assumptions made above. The variation parameters s_1 and s_2 in the FDV-FEM scheme play the role of TVD limiters, Ψ. However, the implicitness parameters s_3 and s_4, beyond the concept of TVD scheme, together with s_1 and s_2, are expected to govern complex physical phenomena such as turbulent boundary layer interactions with shock waves,

finite rate chemistry [with s_5 and s_6 (13.6.5a,b)], widely disparate length and time scales, compressibility effects in high Mach number flows, etc.

(8) PISO and SIMPLE

The basic idea of PISO and SIMPLE is analogous to FDV-FEM in that the pressure correction process is a separate step in PISO or SIMPLE, whereas the concept of pressure correction is implicitly embedded in FDV-FEM by updating the variation parameters based on the upstream and downstream Mach numbers and Reynolds numbers within an element.

The elliptic nature of the pressure Poisson equation in the pressure correction process resembles the terms embedded in the $B_{\alpha\beta rs}$ terms in (13.6.22). Specifically, examine the s_2 terms involving $a_{irq}a_{jsq}$ and $b_{irq}a_{jsq}$ and s_4 term involving $a_{irq}b_{jsq}$. All of these terms are multiplied by $\Phi_{\alpha,i}\Phi_{\beta,j}$ which provide dissipation against any pressure oscillations. Question: Exactly when is such dissipation action needed? This is where the importance of FDV variation parameters based on flowfield parameters comes in. As the Mach number becomes very small (incompressibility effects dominate) the variation parameters s_2 and s_4 calculated from the current flowfield will be indicative of pressure correction required. Notice that a delicate balance between Mach number (s_2 is Mach number dependent) and Reynolds number or Peclet number (s_4 is Reynolds number or Peclet number dependent) is a crucial factor in achieving convergent and stable solutions. Of course, on the other hand, high Mach number flows are also dependent on these variation parameters. In this case all variation parameters, s_1, s_2, s_3, s_4 will play important roles.

16.3 RELATIONSHIPS BETWEEN FEM AND FDV

(1) Taylor-Galerkin Methods (TGM) with Convection and Diffusion Jacobians

Earlier developments for the solution of Navier-Stokes system of equations were based on TGM without using the variation parameters. They can be shown to be special cases of FDV-FEM.

In terms of the both the diffusion Jacobian and the diffusion gradient Jacobian, we write

$$\frac{\partial \mathbf{G}_i}{\partial t} = \mathbf{b}_i \frac{\partial \mathbf{U}}{\partial t} + \mathbf{c}_{ij} \frac{\partial \mathbf{V}_j}{\partial t}$$

with

$$\mathbf{b}_i = \frac{\partial \mathbf{G}_i}{\partial \mathbf{U}}, \qquad \mathbf{c}_{ij} = \frac{\partial \mathbf{G}_i}{\partial \mathbf{V}_j}, \qquad \mathbf{V}_j = \frac{\partial \mathbf{U}}{\partial x_j}$$

Thus, it follows from (13.6.2) with $s_1 = s_3 = s_4 = s_5 = s_6 = 0$ and $s_2 = 1$ that

$$\Delta \mathbf{U}^{n+1} = \Delta t \left(-\frac{\partial \mathbf{F}_i}{\partial x_i} - \frac{\partial \mathbf{G}_i}{\partial x_i} + \mathbf{B} \right)^n + \frac{\Delta t^2}{2} \frac{\partial}{\partial t} \left(-\frac{\partial \mathbf{F}_i}{\partial x_i} - \frac{\partial \mathbf{G}_i}{\partial x_i} + \mathbf{B} \right)^{n+1} + \mathrm{O}(\Delta t^3) \tag{16.3.1}$$

Using the definitions of convection, diffusion, and diffusion rate Jacobians discussed in Section 13.6, the temporal rates of change of the convection and diffusion variables

may be written as follows:

$$\begin{aligned}
\frac{\partial \mathbf{F}_i^n}{\partial t} &= \left(\mathbf{a}_i \frac{\partial \mathbf{U}}{\partial t}\right)^n = \left[\mathbf{a}_i\left(-\frac{\partial \mathbf{F}_j}{\partial x_j} - \frac{\partial \mathbf{G}_j}{\partial x_j} + \mathbf{B}\right)\right]^n \\
\frac{\partial \mathbf{F}_i^{n+1}}{\partial t} &= \mathbf{a}_i\left[\left(-\mathbf{a}_j \frac{\partial}{\partial x_j}(\mathbf{U}^{n+1} - \mathbf{U}^n) - \frac{\partial \mathbf{F}_j^n}{\partial x_j} - \frac{\partial \mathbf{G}_j^{n+1}}{\partial x_j} + \mathbf{B}^{n+1}\right)\right] \\
\frac{\partial \mathbf{G}_i^{n+1}}{\partial t} &= \left(\mathbf{b}_i \frac{\partial \mathbf{U}}{\partial t}\right)^{n+1} + \left[\mathbf{c}_{ij} \frac{\partial}{\partial t}\left(\frac{\partial \mathbf{U}}{\partial x_j}\right)\right]^{n+1}
\end{aligned} \tag{16.3.2}$$

or

$$\frac{\partial \mathbf{G}_i^{n+1}}{\partial t} = \left(\mathbf{b}_i - \frac{\partial \mathbf{c}_{ij}}{\partial x_j}\right)\frac{\Delta \mathbf{U}}{\Delta t}^{n+1} + \frac{\partial}{\partial x_j}\left(\mathbf{c}_{ij}\frac{\Delta \mathbf{U}}{\Delta t}\right)^{n+1} \tag{16.3.3}$$

Substituting (16.3.2) and (16.3.3) into (16.3.1) yields

$$\begin{aligned}
\Delta \mathbf{U}^{n+1} = \Delta t &\left(-\frac{\partial \mathbf{F}_i}{\partial x_i} - \frac{\partial \mathbf{G}_i}{\partial x_i} + \mathbf{B}\right)^n \\
&+ \frac{\Delta t^2}{2}\left\{\frac{\partial}{\partial x_i}\left[-\mathbf{a}_i\left(-\mathbf{a}_j \frac{\partial \Delta \mathbf{U}^{n+1}}{\partial x_j} - \frac{\partial \mathbf{F}_j^n}{\partial x_j} - \frac{\partial \mathbf{G}_j^{n+1}}{\partial x_j} + \mathbf{B}^{n+1}\right)\right.\right. \\
&\left.\left. + \left(\mathbf{e}_i + \frac{\partial \mathbf{c}_{ij}}{\partial x_j}\right)\frac{\Delta \mathbf{U}}{\Delta t}^{n+1} + \frac{\partial \mathbf{B}^{n+1}}{\partial t}\right]\right\}
\end{aligned} \tag{16.3.4}$$

Assuming that

$$\mathbf{e}_i = \mathbf{b}_i - \frac{\partial \mathbf{c}_{ij}}{\partial x_j} \cong 0$$

and neglecting the spatial and temporal derivatives of $\mathbf{B}$, we rewrite (16.3.4) in the form

$$\begin{aligned}
&\left\{1 - \frac{\Delta t^2}{2}\frac{\partial}{\partial x_i}\left(\mathbf{a}_i \mathbf{a}_j - \frac{\mathbf{c}_{ij}}{\Delta t}\right)\frac{\partial}{\partial x_j}\right\}\Delta \mathbf{U}^{n+1} = \mathbf{H}^n \\
&\mathbf{H}^n = \Delta t\left(-\frac{\partial \mathbf{F}_i}{\partial x_i} - \frac{\partial \mathbf{G}_i}{\partial x_i} + \mathbf{B}\right)^n + \frac{\Delta t^2}{2}\frac{\partial}{\partial x_i}\left(\mathbf{a}_i \frac{\partial \mathbf{F}_j}{\partial x_j}\right)^n
\end{aligned} \tag{16.3.5}$$

Here the second derivatives of $\mathbf{G}_i$ are neglected and all Jacobians are assumed to remain constant within an incremental time step but updated at subsequent time steps.

Applying the Galerkin finite element formulation, we have an implicit scheme,

$$\left(\mathbf{A}_{\alpha\beta}\delta_{rs} + \mathbf{B}_{\alpha\beta rs}\right)\Delta \mathbf{U}_{\beta s}^{n+1} = \mathbf{H}_{\alpha r}^n + \mathbf{N}_{\alpha r}^{n+1} + \mathbf{N}_{\alpha r}^n \tag{16.3.6}$$

where

$$\begin{aligned}
\mathbf{B}_{\alpha\beta rs} &= \frac{\Delta t^2}{2}\int_\Omega \left[\left(\mathbf{a}_{irq}\mathbf{a}_{jsq} - \frac{\mathbf{c}_{ijrs}}{\Delta t}\right)\Phi_{\alpha,i}\Phi_{\beta,j}\right]d\Omega \\
\mathbf{H}_{\alpha r}^n &= \Delta t\int_\Omega \left[\Phi_{\alpha,i}\Phi_\beta\left(\mathbf{F}_{\beta ir}^n + \mathbf{G}_{\beta ir}^n\right) + \Phi_\alpha\Phi_\beta \mathbf{B}_{\beta r}^n - \frac{\Delta t}{2}\mathbf{a}_{irs}\Phi_{\alpha,i}\Phi_{\beta,j}\mathbf{F}_{\beta js}^n\right]d\Omega \\
\mathbf{N}_{\alpha r}^{n+1} &= \frac{\Delta t^2}{2}\int_\Gamma \left(\mathbf{a}_{irq}\mathbf{a}_{jsq} - \frac{\mathbf{c}_{ijrs}}{\Delta t}\right)\overset{*}{\Phi}_\alpha \Delta \mathbf{U}_{s,j}^{n+1} n_i d\Gamma \\
\mathbf{N}_{\alpha r}^n &= -\int_\Gamma \left[\Delta t\overset{*}{\Phi}_\alpha\left(\mathbf{F}_{ir}^n + \mathbf{G}_{ir}^n\right) - \frac{\Delta t^2}{2}\mathbf{a}_{irs}\overset{*}{\Phi}_\alpha \mathbf{F}_{js,j}^n\right]n_i d\Gamma
\end{aligned}$$

Here we note that the algorithm given by (16.3.6) results from (13.6.20) in FDV by setting $s_1 = s_3 = s_4 = 0, s_2 = 1, b_{irq}a_{jsq} = c_{ijrs}/\Delta t$, and neglecting the terms with b_{jrs} and derivatives of $\mathbf{G}_i$ and $\mathbf{B}$, the form identical to that introduced in Section 13.2.1.

(2) Taylor Galerkin Methods (TGM) with Convection Jacobians

Diffusion Jacobians may be neglected if their influence is negligible. In this case the Taylor-Galerkin finite element analog may be derived using only the convective Jacobian from the Taylor series expansion,

$$\mathbf{U}^{n+1} = \mathbf{U}^n + \Delta t \frac{\partial \mathbf{U}^n}{\partial t} + \frac{\Delta t^2}{2}\frac{\partial^2 \mathbf{U}^n}{\partial t^2} + \mathrm{O}(\Delta t^3) \tag{16.3.7}$$

where

$$\frac{\partial \mathbf{U}}{\partial t} = -\frac{\partial \mathbf{F}_i}{\partial x_i} - \frac{\partial \mathbf{G}_i}{\partial x_i} + \mathbf{B} = -\mathbf{a}_i \frac{\partial \mathbf{U}}{\partial x_i} - \frac{\partial \mathbf{G}_i}{\partial x_i} + \mathbf{B} \tag{16.3.8}$$

$$\frac{\partial^2 \mathbf{U}}{\partial t^2} = -\frac{\partial}{\partial t}\left(\mathbf{a}_i \frac{\partial \mathbf{U}}{\partial x_i} + \frac{\partial \mathbf{G}_i}{\partial x_i} - \mathbf{B}\right)$$

or

$$\frac{\partial^2 \mathbf{U}}{\partial t^2} = \frac{\partial}{\partial x_j}\left(\mathbf{a}_i \mathbf{a}_j \frac{\partial \mathbf{U}}{\partial x_i}\right) + \frac{\partial}{\partial x_i}\left(\mathbf{a}_i \frac{\partial \mathbf{G}_j}{\partial x_j}\right) - \frac{\partial}{\partial x_i}(\mathbf{a}_i \mathbf{B}) + \frac{\partial \mathbf{B}}{\partial t} \tag{16.3.9}$$

Substituting (16.3.8) and (16.3.9) into (16.3.7), we obtain

$$\Delta \mathbf{U}^{n+1} = \Delta t \left\{ -\frac{\partial \mathbf{F}_i}{\partial x_i} - \frac{\partial \mathbf{G}_i}{\partial x_i} + \mathbf{B} + \frac{\Delta t}{2}\left[\frac{\partial}{\partial x_j}\left(\mathbf{a}_i \mathbf{a}_j \frac{\partial \mathbf{U}}{\partial x_i}\right) + \frac{\partial^2 (\mathbf{a}_i \mathbf{G}_j)}{\partial x_i \partial x_j} + \frac{\partial}{\partial x_i}(\mathbf{a}_i \mathbf{B}) + \frac{\partial \mathbf{B}}{\partial t} \right] \right\}^n \tag{16.3.10a}$$

Expanding $\partial \mathbf{F}_j / \partial t$ at $(n+1)$ time step

$$\frac{\partial \mathbf{F}_i^{n+1}}{\partial t} = \left[\mathbf{a}_i \left(-\frac{\partial \mathbf{F}_j}{\partial x_j} - \frac{\partial \mathbf{G}_j}{\partial x_j} + \mathbf{B}\right)\right]^{n+1} = \mathbf{a}_i^{n+1}\left[-\mathbf{a}_j \frac{\partial \Delta \mathbf{U}^{n+1}}{\partial x_j} - \frac{\partial \mathbf{F}_j^n}{\partial x_j} - \frac{\partial \mathbf{G}_j^{n+1}}{\partial x_j} + \mathbf{B}^{n+1}\right]$$

and substituting the above into (16.3.7–16.3.9), we arrive at $\Delta \mathbf{U}^{n+1}$ in a form different from (16.3.10a):

$$\Delta \mathbf{U}^{n+1} = \Delta t \left(-\frac{\partial \mathbf{F}_i}{\partial x_i} - \frac{\partial \mathbf{G}_i}{\partial x_i} + \mathbf{B}\right)^n + \frac{\Delta t^2}{2}\left\{ \frac{\partial}{\partial x_i}\left(\mathbf{a}_i \mathbf{a}_j \frac{\partial \Delta \mathbf{U}^{n+1}}{\partial x_j} + \mathbf{a}_i \frac{\partial \mathbf{F}_j^n}{\partial x_j}\right) + \frac{\partial^2 (\mathbf{a}_i \mathbf{G}_j)^{n+1}}{\partial x_i \partial x_j} + \frac{\partial}{\partial x_i}(\mathbf{a}_i \mathbf{B})^{n+1} + \frac{\partial \mathbf{B}^{n+1}}{\partial t} \right\} \tag{16.3.10b}$$

$$\mathbf{H}^n = \left[1 - \frac{\Delta t^2}{2}\frac{\partial}{\partial x_i}\left(\mathbf{a}_i \mathbf{a}_j - \frac{\mathbf{c}_{ij}}{\Delta t}\right)\frac{\partial}{\partial x_j}\right]\Delta \mathbf{U}^{n+1} \tag{16.3.10c}$$

$$\mathbf{H}^n = \Delta t \left(-\frac{\partial \mathbf{F}_i}{\partial x_i} - \frac{\partial \mathbf{G}_i}{\partial x_i} + \mathbf{B}\right)^n + \frac{\Delta t^2}{2}\frac{\partial}{\partial x_i}\left(\mathbf{a}_i \frac{\partial \mathbf{F}_j}{\partial x_j}\right)^n$$

where second derivatives of $\mathbf{G}_i$ are assumed to be negligible and $\mathbf{B}$ is constant in space

and time, arriving at an implicit finite element scheme,

$$(\mathbf{A}_{\alpha\beta}\delta_{rs} + \mathbf{B}_{\alpha\beta rs})\,\Delta\mathbf{U}_{\beta s}^{n+1} = \mathbf{H}_{\alpha r}^{n} + \mathbf{N}_{\alpha r}^{n+1} + \mathbf{N}_{\alpha r}^{n} \tag{16.3.11}$$

where

$$\mathbf{A}_{\alpha\beta} = \int_{\Omega} \Phi_{\alpha}\Phi_{\beta}\, d\Omega$$

$$\mathbf{B}_{\alpha\beta rs} = \frac{\Delta t^2}{2}\int_{\Omega}\left[\left(\mathbf{a}_{irq}\mathbf{a}_{jsq} - \frac{\mathbf{c}_{ijrs}}{\Delta t}\right)\Phi_{\alpha,i}\Phi_{\beta,j}\right]d\Omega$$

$$\mathbf{H}_{\alpha r}^{n} = \Delta t\int_{\Omega}\left[\Phi_{\alpha,i}\Phi_{\beta}\left(\mathbf{F}_{\beta ir}^{n} + \mathbf{G}_{\beta ir}^{n}\right) - \Phi_{\alpha}\Phi_{\beta}\mathbf{B}_{\beta r}^{n} - \frac{\Delta t^2}{2}\mathbf{a}_{irs}\Phi_{\alpha,i}\Phi_{\beta,j}\mathbf{F}_{\beta js}^{n}\right]d\Omega$$

$$\mathbf{N}_{\alpha r}^{n+1} = \frac{\Delta t^2}{2}\int_{\Gamma}\left(\mathbf{a}_{irq}\mathbf{a}_{jsq} - \frac{\mathbf{c}_{ijrs}}{\Delta t}\right)\overset{*}{\Phi}_{\alpha}\Delta\mathbf{U}_{s,j}^{n+1} n_i\, d\Gamma$$

$$\mathbf{N}_{\alpha r}^{n} = -\int_{\Gamma}\left[\Delta t\,\overset{*}{\Phi}_{\alpha}\left(\mathbf{F}_{ir}^{n} + \mathbf{G}_{ir}^{n}\right) - \frac{\Delta t^2}{2}\mathbf{a}_{irs}\,\overset{*}{\Phi}_{\alpha}\mathbf{F}_{js,j}^{n}\right]n_i\, d\Gamma$$

It should be noted that the form (16.3.10c) arises from (13.6.20) in FDV with $s_1 = s_3 = s_4 = b_j = 0$ and $s_2 = 1$, an algorithm similar to TGM introduced in Section 13.2.1.

(3) Generalized Petrov-Galerkin

The Generalized Petrov-Galerkin (GPG) method can be identified in FDV by setting $s_1 = s_2 = 1, s_3 = s_4 = 0, \mathbf{b}_i = \mathbf{c}_{ij} = \mathbf{d} = 0, \mathbf{Q}^n = 0, \mathbf{E}_i = \mathbf{a}_i$, and $\mathbf{E}_{ij} = \frac{1}{2}\Delta t^2\mathbf{a}_i\mathbf{a}_j$, so that (13.6.20) takes the form

$$\frac{\Delta\mathbf{U}}{\Delta t} + \mathbf{a}_i\frac{\partial\Delta\mathbf{U}}{\partial x_i} - \frac{\Delta t}{2}\mathbf{a}_i\mathbf{a}_j\frac{\partial^2\Delta\mathbf{U}}{\partial x_i\partial x_j} = 0 \tag{16.3.12}$$

For the steady-state nonincremental form in 1-D, we write (16.3.12) in the form

$$a\frac{\partial u}{\partial x} - \Delta t\frac{a^2}{2}\frac{\partial^2 u}{\partial x^2} = 0 \tag{16.3.13}$$

Taking the Galerkin integral of (16.3.13) leads to

$$\int \Phi_N^{(e)}\left(a\frac{\partial u}{\partial x} - \Delta t\frac{a^2}{2}\frac{\partial^2 u}{\partial x^2}\right)dx = 0, \qquad \int W_N^{(e)} a\frac{\partial u}{\partial x}dx = 0 \tag{16.3.14}$$

for vanishing Neumann boundaries. Here $W_N^{(e)}$ is the Petrov-Galerkin test function,

$$W_N^{(e)} = \Phi_N^{(e)} + \alpha h\frac{\partial\Phi_N^{(e)}}{\partial x} \tag{16.3.15}$$

with $\alpha = C/2$ and $C = a\Delta t/\Delta x$ being the Courant number.

For isoparametric coordinates in two dimensions, the Petrov-Galerkin test function assumes the form

$$W_N^{(e)} = \Phi_N^{(e)} + \beta g_i\frac{\partial\Phi_N^{(e)}}{\partial x} \tag{16.3.16}$$

with

$$\beta = \frac{1}{4}(\overline{\alpha}_\xi h_\xi + \overline{\alpha}_\eta h_\eta)$$

$$\overline{\alpha}_\xi = \coth\left(\frac{R_\xi}{2}\right) - \frac{2}{R_\xi}, \qquad \overline{\alpha}_\eta = \coth\left(\frac{R_\eta}{2}\right) - \frac{2}{R_\eta}$$

$$g_i = \frac{v_i}{\sqrt{v_j v_j}}$$

where R_ξ is the Reynolds number or Peclet number in the direction of isoparametric coordinates (ξ, η). Note that the GPG process given by (16.3.12)–(16.3.16) leads to the streamline upwinding Petrov-Galerkin (SUPG) scheme as a special case, thus leading to the analogy between FDV and GPG.

16.4 OTHER METHODS

We have examined in the previous chapters most of the currently available CFD methods. Throughout this text, it was intended that the reader be given adequate information so that he/she could make a final decision to choose the most suitable method for the problem at hand. Though biases or preferences in choosing CFD methods are often common among practitioners, this text may still serve as a guide and possibly toward re-orientation. It was shown that FVM can be formulated from either FDM or FEM. The FDV methods discussed in Chapters 6 and 13 as well as other methods are expected to meet these challenges. In particular, the ability of FDV methods to generate other prominent CFD schemes has been demonstrated. In the past, numerical methods other than those presented in the previous chapters have been used also. Among them are the boundary element methods (BEM), coupled Eulerian-Lagrangian (ECL) methods, particle-in-cell (PIC) methods, and Monte Carlo methods (MCM). The detailed coverage of these topics is beyond the scope of this book; but, for the sake of historical perspectives, we shall briefly review them next.

16.4.1 BOUNDARY ELEMENT METHODS

The boundary element methods (BEM) are based on boundary integral equations in which only the boundaries of a region are used to obtain apparoximate solutions. Interpolation functions for the surface behavior are coupled with the solutions to the governing equations which apply over the domain. The resulting equations are solved numerically for values on the boundary alone, and values at interior points are calculated subsequently from the surface data.

It is thus clear that fewer equations are involved in the solution by the BEM. On the other hand, it is required that the governing equations be linear but this can be overcome by linearization through Kirchhoff transformation [Brebbia, 1978; Brebbia, Telles, and Wrobel, 1983].

Green's Function and Boundary Integral Equation

To illustrate, let us consider the Laplace equation,

$$\nabla^2 \phi = 0 \tag{16.4.1}$$

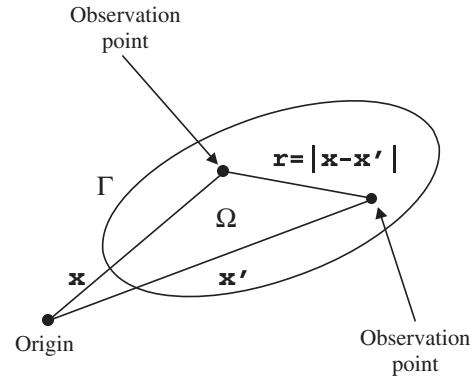

Figure 16.4.1 Location of source and field points.

Assume a weighting function ψ and the weighted residual integral of (16.4.1) such that

$$\int_{\Omega} \psi \nabla^2 \phi d\Omega = 0 \tag{16.4.2}$$

Integrating this by parts twice,

$$\int_{\Omega} (\psi \nabla^2 \phi - \phi \nabla^2 \psi) d\Omega = \int_{\Gamma} [\psi (\mathbf{n} \cdot \nabla \phi) - \phi (\mathbf{n} \cdot \nabla \psi)] d\Gamma \tag{16.4.3}$$

It follows from (16.4.1) and (16.4.2) that

$$\int_{\Omega} \phi \nabla^2 \psi \, d\Omega = \int_{\Gamma} \left(\phi \frac{\partial \psi}{\partial n} - \psi \frac{\partial \phi}{\partial n} \right) d\Gamma = 0 \tag{16.4.4}$$

which is known as the Green's identity. Here, the weighting function ψ is denoted as the Green's function, $G(\mathbf{x}'|\mathbf{x})$, which is assumed to be the solution of

$$\nabla^2 G(\mathbf{x}'|\mathbf{x}) = \delta(\mathbf{x}' - \mathbf{x}) \tag{16.4.5}$$

where $\delta(\mathbf{x}' - \mathbf{x})$ is the Dirac delta function with $\mathbf{x}$ and $\mathbf{x}'$ being the source point and the observation point, respectively, such that (Figure 16.4.1)

$$\int_{\Omega} \phi(\mathbf{x}) \delta(\mathbf{x}' - \mathbf{x}) d\Omega = \phi(\mathbf{x}') \tag{16.4.6}$$

For a polar coordinate system (r, θ), it can easily be shown that the solution of (16.4.5) is of the form

$$G = \frac{1}{2\pi} \ln r \tag{16.4.7}$$

or, for a three-dimensional domain,

$$G = \frac{1}{4\pi r} \tag{16.4.8}$$

The fundamental solutions for other types of partial differential equations are as follows:

Helmholtz Equations

$$\nabla^2 G + k^2 G = \delta(\mathbf{x}' - \mathbf{x}) \tag{16.4.9}$$

$$G = \frac{1}{4\pi} \frac{e^{ikr}}{r} \quad \text{for } 3\text{-}D$$

Diffusion Equations

$$\frac{\partial G}{\partial t} - a\nabla^2\phi = \delta(\mathbf{x}' - \mathbf{x})\delta(t' - t) \tag{16.4.10}$$

$$G = \frac{1}{(4\pi a\tau)^{d/2}} \exp\left(-\frac{r^2}{4\pi\tau}\right)$$

where $\tau = t' - t$ and d denotes the spatial dimension. The fundamental solution represents the effect of the unit point source applied at the observation point $\mathbf{x}'$ on the source point $\mathbf{x}$ in an infinite region.

To illustrate applications, consider the governing equation for an unsteady heat conduction problem:

$$\frac{\partial T}{\partial t} - aT_{,ii} - \frac{Q}{\rho c} = 0 \tag{16.4.11}$$

subject to boundary conditions

$$\begin{aligned} T &= T_1 && \text{on } \Gamma_1 \\ -kT_{,i}n_i &= q_2 && \text{on } \Gamma_2 \\ -kT_{,i}n_i &= \overline{\alpha}(T_3 - T') && \text{on } \Gamma_3 \end{aligned}$$

Recast (16.4.11) in terms of Green's identity and integrate with respect to time,

$$\beta T = \int_0^{t'}\int_\Gamma (aT_{,i}n_i - aTG_{,i}n_i)d\Gamma dt + \int_0^{t'}\int_\Omega \frac{Q}{\rho c} G d\Omega dt + \int_\Omega TG\Big|_{t=0} \tag{16.4.12}$$

Introducing the interpolation functions in the form,

$$T = \Phi_\alpha T_\alpha$$

$$q = \Phi_\alpha q_\alpha$$

and rewriting (16.4.12) using the above approximations, we obtain

$$A_{\alpha\beta}^{(n+1)} T_\beta^{(n+1)} = F_\alpha^{(n)} \tag{16.4.13}$$

where

$$F_\alpha^n = B_{\alpha\beta}^{(n+1)} q_\beta^{(n+1)} + A_{\alpha\beta}^{(n)} T_\beta^{(n)} + B_{\alpha\beta}^{(n)} q_\beta^{(n)} + C_\alpha^{(\Gamma)} + C_\alpha^{\Omega}$$

$$A_{\alpha\beta}^{(n+1)} = \frac{1}{2}\delta_{\alpha\beta} - A_{\alpha\beta}^* \quad \text{for smooth boundary}$$

$$A_{\alpha\beta}^* = -\int_0^{t'}\left[\int_{\Gamma_2} a(G_{,i}n_i)_\alpha \Phi_\beta d\Gamma - \int_{\Gamma_3} a(G_{,i}n_i)_\alpha \Phi_\beta d\Gamma\right]dt$$

$$B_{\alpha\beta} = \int_0^t \int_{\Gamma_1} a(G)_\alpha \Phi_\beta d\Omega$$

$$C_\alpha^{(\Gamma)} = \int_0^{t'}\left[\int_{\Gamma_2} \frac{-q_{\Gamma_2}}{\rho c}(G)_\alpha d\Gamma - \int_{\Gamma_3} \frac{\overline{\alpha}}{\rho c}(T_{\Gamma_3} - T')d\Gamma\right]dt + \int_0^{t'}\int_\Omega (G)_\alpha \frac{1}{\rho c}\Phi_\beta Q_\beta d\Omega dt$$

$$C_\alpha^{(\Omega)} = \int_\Omega (G)_\alpha \Phi_\beta T_\beta d\Omega|_{t=0}$$

Since the algebraic equations given by (16.4.13) are linear, the solution involves a simple marching in time until desired time is reached.

16.4.2 COUPLED EULERIAN-LAGRANGIAN METHODS

It should be pointed out that all methods introduced in the previous chapters are based on the Eulerian coordinates in which computational nodes are fixed in space and all variables are calculated at these fixed nodes. In some instances in reality, however, it is of interest to compute variables in the Lagrangian coordinates where the mesh points are allowed to move along with the fluid particles. Furthermore, it is often convenient to have both Eulerian and Lagrangian coordinates coupled, known as the coupled Eulerian-Lagrangian (CEL) methods, useful in highly distorted flows or multiphase flows. Precise mathematical representations and treatments of Eulerian and Lagrangian coordinates are presented in Chung [1996].

The CEL methods were first developed by Noh [1964]. The basic idea is that the boundary Γ of the region Ω given by

$$\Omega = \bigcup_{i=1}^{n} \Omega_i$$

and the curves D_i which separate the subregions Ω_i are to be approximated by time-dependent Lagrangian lines $L_i(t)$. A subregion R_i which is approximated by the time-independent Eulerian mesh E will consequently have its boundary Γ_i prescribed by the Lagrangian calculations. Thus, the Eulerian calculation reduces to a calculation on a fixed mesh having a prescribed moving boundary and therefore contributes one of the central calculations in the CEL methods. The calculations that are made at each time step are divided into three main parts: Lagrange calculations, Eulerian calculations, and a calculation that couples the Eulerian and Lagrangian regions by defining that part of the Eulerian mesh which is active and by determining the pressures from the Eulerian region which act on the Lagrangian boundaries.

Physically, the local sound speed (and fluid velocity) can vary considerably in different regions of the fluid, and the mesh size in general will also be a function of the region being approximated. It is therefore to be expected that the different subregions will have different stability requirements. Thus, it is desirable to allow these different regions their characteristic time interval in hydrodynamic calculations. Approximations for difference equations for Eulerian coordinates (Figure 16.4.2a) and Lagrangian coordinates (Figure 16.4.2b) are given below.

Eulerian Difference Equations

The differential equations for Eulerian coordinates are the same as given in Chapter 2. To obtain finite difference equations for the above equations, we first introduce the following definitions:

$$\text{(i)}\quad u_{k+1,l+1}^{n+1} = \frac{1}{2}\left(u_{k+1,l}^{n+1/2} + u_{k+1,l+1}^{n+1/2}\right) \tag{16.4.14a}$$

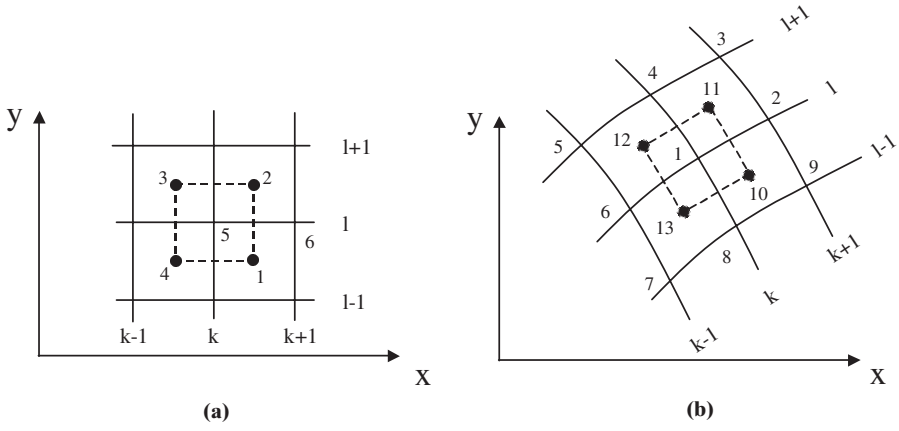

Figure 16.4.2 Eulerian and Lagrangian descriptions. **(a)** Eulerian description. **(b)** Lagrangian description.

$$\text{(ii)}\quad v_{k+1,l+1}^{n+1} = \frac{1}{2}\left(u_{k+1,l+1}^{n+1/2} + u_{k+1,l+1}^{n+1/2}\right) \tag{16.4.14b}$$

$$\text{(iii)}\quad (fu\Delta y)_{k+1,l+1}^{n+1/2} = \begin{cases} f_{k+1,l+1/2}^{n} u_{k+1,l+1/2}^{n+1/2}(y_{l+1} - y_l) & \text{if } u_{k+1,l+1/2}^{n+1/2} \geq 0 \\ f_{k+1,l+3/2}^{n} u_{k+1,l+1/2}^{n+1/2}(y_{l+1} - y_l) & \text{if } u_{k+1,l+1/2}^{n+1/2} \leq 0 \end{cases} \tag{16.4.14c}$$

$$\text{(iv)}\quad (f\nu\Delta x)_{k+1,l+1}^{n+1/2} = \begin{cases} f_{k+1,l+1/2}^{n} u_{k+1,l+1/2}^{n+1/2}(x_{k+1} - x_k) & \text{if } \nu_{k+1,l+1/2}^{n+1/2} \geq 0 \\ f_{k+1,l+3/2}^{n} u_{k+1,l+1/2}^{n+1/2}(x_{k+1} - y_k) & \text{if } \nu_{k+1,l+1}^{n+1} \leq 0 \end{cases} \tag{16.4.14d}$$

$$\text{(v)}\quad (\boldsymbol{\nabla} \cdot f\mathbf{U})_{k+1,l+1}^{n+1}$$
$$= \frac{(fu\Delta y)_{k+1,l+1/2}^{n+1/2} + (f\nu\Delta x)_{k+1/2,l+1}^{n+1/2} - (fu\Delta y)_{k,l+1/2}^{n+1/2} + (f\nu\Delta x)_{k+1/2,l}^{n+1/2}}{(x_{k+1} - x_k)(y_{l+1} - y_l)} \tag{16.4.14e}$$

$$\text{(vi)}\quad \left(\frac{\Delta \overline{p}}{\Delta x}\right)_{k,l}^{n} = \frac{1}{2}\frac{\overline{p}_1^n + \overline{p}_2^n - \overline{p}_3^n - \overline{p}_4^n}{x_1 - x_4} \tag{16.4.15a}$$

$$\text{(vii)}\quad \left(\frac{\Delta \overline{p}}{\Delta y}\right)_{k,l}^{n} = \frac{1}{2}\frac{\overline{p}_2^n + \overline{p}_3^n - \overline{p}_1^n - \overline{p}_4^n}{y_2 - y_1} \tag{16.4.15b}$$

$$\text{(viii)}\quad (fu\Delta y)_{k+1/2,l}^{n-1} = (y_2 - y_1)\frac{\left(u_5^{n-1/2} + u_6^{n-1/2}\right)}{2} \begin{cases} f_5^{n-1} & \text{if } \left(u_5^{n-1/2} u_6^{n-1/2}\right) \geq 0 \\ f_6^{n-1} & \text{if } \left(u_5^{n-1/2} u_6^{n-1/2}\right) \leq 0 \end{cases} \tag{16.4.15c}$$

$$\text{(ix)}\quad (f\nu\Delta x)_{k/2,l+1}^{n-1/2} = (x_2 - x_3)\frac{\left(\nu_5^{n-1/2} + \nu_7^{n-1/2}\right)}{2} \begin{cases} f_5^{n-1} & \text{if } \left(\nu_5^{n-1/2} u_7^{n-1/2}\right) \geq 0 \\ f_7^{n-1} & \text{if } \left(\nu_5^{n-1/2} \nu_7^{n-1/2}\right) \leq 0 \end{cases} \tag{16.4.15d}$$

$$\text{(x)}\quad (\nabla\cdot f\mathbf{U})^{n-1}_{k,l} = \frac{(fu\Delta y)^{n-1/2}_{k+1,l} + (fv\Delta x)^{n-1/2}_{k,l+1/2} - (fu\Delta y)^{n-1/2}_{k-1/2,l} + (fv\Delta x)^{n-1/2}_{k/2,l-1/2}}{(x_1 - x_4)(y_2 - y_1)} \tag{16.4.15e}$$

with $\overline{p} = p + q, \qquad q = \frac{1}{2}\rho v_i v_i.$

Based on the above definitions, the finite difference equations for inviscid flows are of the form:

Continuity

$$\rho^{n+1}_{k+1/2,l+1/2} = \rho^{n}_{k+1/2,l+1/2} - \Delta t(\nabla\cdot\rho\mathbf{U})^{n+1/2}_{k+1/2,l+1/2} \tag{16.4.16}$$

Momentum

$$M^{n+1/2}_{k,l} = M^{n-1/2}_{k,l} - \Delta t\left[(\nabla\cdot M\mathbf{U})^{n-1/2}_{k,l} + \left(\frac{\Delta\overline{p}}{\Delta x}\right)^{n}_{k,l}\right], \quad M = \rho u \tag{16.4.17a}$$

$$N^{n+1/2}_{k,l} = M^{n-1/2}_{k,l} - \Delta t\left[(\nabla\cdot M\mathbf{U})^{n-1/2}_{k,l} + \left(\frac{\Delta\overline{p}}{\Delta y}\right)^{n}_{k,l}\right], \quad N = \rho v \tag{16.4.17b}$$

Energy

$$\varepsilon^{n+1}_{k+1/2,l+1/2} = \varepsilon^{n}_{k+1/2,l+1/2} - \Delta t\Big[(\nabla\cdot\varepsilon U)^{n+1/2}_{k+1/2,l+1/2} + (\overline{p})^{n+1/2}_{k+1/2,l+1/2} + q^{n+1/2}_{k+1/2,l+1/2}(\nabla\cdot\mathbf{U})^{n+1/2}_{k+1/2,l+1/2}\Big] \tag{16.4.18}$$

Lagrangian Difference Equations

The differential equations in Lagrangian coordinates are given by

$$\frac{\partial u}{\partial t} = -\frac{1}{\rho}\frac{\partial p}{\partial x}, \quad \frac{\partial v}{\partial t} = -\frac{1}{\rho}\frac{\partial p}{\partial y} \tag{16.4.19}$$

$$u = \frac{\partial x}{\partial t}, \quad v = \frac{\partial y}{\partial t} \tag{16.4.20}$$

$$\rho J = const., \qquad \frac{\partial\varepsilon}{\partial t} = \frac{p}{\rho^2}\frac{\partial\rho}{\partial t}, \qquad p = p(\varepsilon,\rho) \tag{16.4.21}$$

with J being the Jacobian between the cartesian and curvilinear coordinates (Figure 16.4.2b).

The Lagrangian difference equations corresponding to (16.4.19–21) are written as follows.

$$u^{n+1}_{k,l} = u^{n-1/2}_{k,l} - \Delta t\frac{(\overline{p}, y)^{n}_{k,l}}{(\rho J)_{k,l}} \tag{16.4.22a}$$

$$v^{n+1}_{k,l} = v^{n-1/2}_{k,l} - \Delta t\frac{(\overline{p}, y)^{n}_{k,l}}{(\rho J)_{k,l}} \tag{16.4.22b}$$

$$x^{n+1}_{k,l} = x^{n}_{k,l} + \Delta t u^{n+1}_{k,l} \tag{16.4.23a}$$

$$y^{n+1}_{k,l} = y^{n}_{k,l} + \Delta t u^{n+1}_{k,l} \tag{16.4.23b}$$

$$\rho^{n+1}_{k+1.l+1} = \rho^{n}_{k+1/2.l+1/2} \frac{J^{n}_{k+1/2.l+1/2}}{J^{n+1/2}_{k+1/2.l+1/2}} \tag{16.4.24}$$

$$\varepsilon^{n+1}_{k+1.l+1} = \varepsilon^{n}_{k+1/2.l+1/2} + \overline{p}^{n+1/2}_{k+1/2.l+1/2} \frac{(\rho^{n+1} - \rho^{n})_{k+1/2.l+1/2}}{\rho^{n+1}\rho^{n}_{k+1/2.l+1/2}} \tag{16.4.25}$$

The velocity equations (16.4.23a,b) must be modified for the points of the lattice which define the boundaries of the Lagrangian region, but the remaining equations hold for all points of the mesh.

Finite elements have been used in CEL methods as applied to multiphase flows. Surface tension on the interfaces between different fluids can also be taken into account. These and other topics using CEL are discussed in Chapter 25.

16.4.3 PARTICLE-IN-CELL (PIC) METHOD

This is one of the early methods developed in the Los Alamos Scientific Laboratory in dealing with highly distorted flows with slippages or colliding interfaces [Evans and Harlow, 1957; Harlow, 1964]. In this method, Eulerian mesh is used and the cell is filled with particles of the same kind or a mixture of different kinds. The calculation of changes in the fluid configuration proceeds through a series of time steps or cycles. Each cell is characterized by a set of variables describing the mean components of velocity, the internal energy, the density, and the pressure in the cell. In the Eulerian part of the calculations, only the cellwise quantities are changed and the fluid is assumed to be momentarily completely at rest. In order to accomplish the particle motion, it is convenient to prepare as a first step for the possibility of particles moving across cell boundaries. For this purpose, the specific quantities in each of the cells are transformed to cellwise totals.

The results of a calculation applied to the formation of a crater by an explosion in an atmosphere above a dense material are shown in Figure 16.4.3 [Harlow, 1964]. The initial one for time $t = 0$ shows cold ground above which is a small and intensely heated sphere in an otherwise cold atmosphere. The second frame, two time units later, is shown in order to demonstrate the intense packing of particles in the initially heated sphere. The third frame shows a strong shock in the ambient atmosphere, together with considerable depression of the ground. The final frame shows, at time sixty units, the configuration just before the particles began to fall off the computation regions.

16.4.4 MONTE CARLO METHODS (MCM)

Monte Carlo methods have been successfully used in many problems in physics and engineering where stochastic or statistical approaches can describe the physical phenomena more realistically [Hammersley and Handscomb, 1964; Binder, 1984]. They have been extensively applied to electron distributions, neutron diffusion, radiative heat transfer, probability density functions for turbulent microscale eddies, etc.

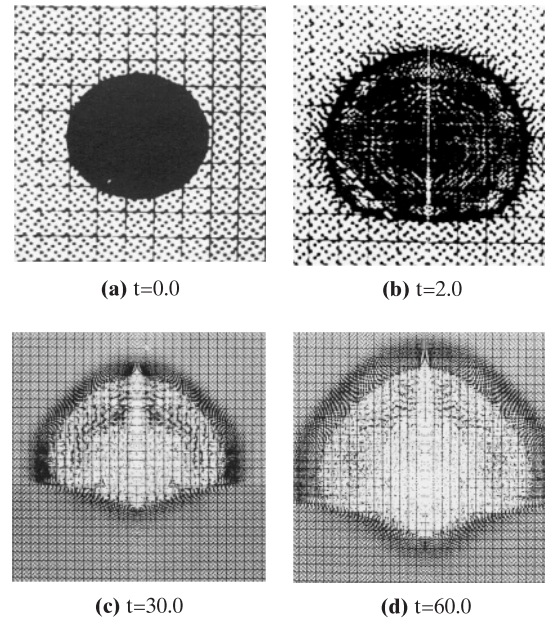

(a) t=0.0 **(b)** t=2.0

(c) t=30.0 **(d)** t=60.0

Figure 16.4.3 Configurations of particles at four times in the crater formulation problem; grid lines show every other cell boundary [Harlow, 1964].

In general, the Monte Carlo method is a statistical approach to the solution of multiple integrals of the type

$$I(\xi_1, \xi_2, \ldots\ldots, \xi_k) = \int_0^1 \int_0^1 w(\xi_1, \xi_2, \ldots\ldots, \xi_k) dP_1(\xi_1) dP_2(\xi_2) \ldots\ldots dP_k(\xi_k) \tag{16.4.26}$$

Monte Carlo becomes indispensable whenever multiple integrals have variables and can not be evaluated efficiently by standard numerical techniques.

As an example, let us consider the heat conduction equation,

$$\frac{\partial^2 T}{\partial x^2} + \frac{\partial^2 T}{\partial y^2} = 0$$

The integral (16.4.26) corresponding to heat conduction may be written as

$$I(\xi) = \int_0^1 w(\xi_1) dP_1(\xi_1) \tag{16.4.27}$$

In terms of the finite difference discretization, the integral (16.4.27) represents a finite difference equation written for the temperature at nodes (i, j) as

$$T_{i,j} = P_{x^+} T_{i+1,j} + P_{y^+} T_{i,j+1} + P_{x^-} T_{i-1,j} + P_{y^-} T_{i,j-!} \tag{16.4.28}$$

with

$$P_{x^+} = P_{x^-} = \frac{\Delta y/\Delta x}{2(\Delta y/\Delta x + \Delta x/\Delta y)} \tag{16.4.29a}$$

$$P_{y^+} = P_{y^-} = \frac{\Delta x/\Delta y}{2(\Delta y/\Delta x + \Delta x/\Delta y)} \tag{16.4.29b}$$

The procedure described above is often known as the random walk. In this simple example, the Monte Carlo approximations for heat conduction resembles the four-point FDM. In conduction, an abstraction using particles or random walks is used to simulate a solution of a partial differential equation, whereas in radiation a physical phenomenon – the transfer of photons – is simulated.

16.5 SUMMARY

In this chapter, we have revisited the finite difference methods and finite element methods. The emphasis has been to show their analogies. In this process, differences between these two major computational methods have been recognized. The advantage of studying both methods on an equal footing has been stressed. The finite volume methods based on either FDM or FEM are increasingly popular in applications to many engineering projects. Example problems in Part Five will demonstrate these trends.

Computational methods other than FDM, FEM, and FVM have been briefly reviewed, including boundary element methods, coupled Eulerian-Lagrangian methods, particle-in-cell methods, and Monte Carlo methods. Detailed presentations of these methods are beyond the scope of this book. In fact, the topics covered in this chapter alone could have been dealt with in an independent part.

As we look back on the chapters in Part Two and Part Three, our focus has been to introduce to the reader what has been accomplished in CFD for the past century. It was not possible to cover all minute details of every method that was introduced. Pertinent references are provided at the end of each chapter. Obviously, the reader should consult these references for further guidance.

This chapter marks the end of Parts Two and Three, including FDM, FEM, and FVM, but we have not discussed other important subjects: automatic grid generation, adaptive methods, and computing techniques. We shall examine them in the next several chapters, Part Four.

REFERENCES

Binder, K. [1984]. *Applications of the Monte Carlo Method in Statistical Physics*. Berlin: Springer-Verlag.

Brebbia, C. A. [1978]. *The Boundary Element Method for Engineers*. London: Pentech Press.

Brebbia, C. A., Telles, J., and Wrobel, L. [1983]. *Boundary Element Methods – Theory and Applications*. New York: Springer-Verlag.

Chung, T. J. [1996]. *Applied Continuum Mechanics*. London: Cambridge University Press.

Evans, M. W. and Harlow, F. H. [1957]. The particle-in-cell method for hydrodynamic calculations. Los Alamos Scientific Laboratory Report No. LA-2139.

Hammersley, J. M. and Handscomb, D. C. [1964]. *Monte Carlo Methods*. London: Methuen.

Harlow, F. H. [1964]. The particle-in-cell computing method for fluid dynamics. In F. H. Harlow, (ed.). *Methods in Computational Physics*. New York: Academic Press.

Noh, W. F. [1964]. CEL: A time-dependent, two-space-dimensional, coupled Eulerian-Lagrange code. In F. H. Harlow (ed.). *Methods in Computational Physics*. New York: Academic Press.